Anal. Bioanal. Electrochem., Vol. 14, No. 2, 2022, 216-227

Analytical & Bioanalytical Electrochemistry

2022 by CEE
www.abechem.com

Full Paper

Comparison of Corrosion Behavior between Fine-Grained and Coarse-grained Fe-18.5% Cr Ferritic Stainless Steel in 0.01 M NaOH Solution

Hadi Irani,[1] and Mehdi Shaban Ghazani[2],*

[1]Faculty of Materials Science Engineering, Sahand University of Technology, P.O. Box: 51335-1996, Tabriz, Iran

[2]Department of Materials Science Engineering, University of Bonab, P.O. Box: 5551761167, Bonab, Iran

*Corresponding Author, Tel.: +989104000567

E-Mail: m_shaban@ubonab.ac.ir

Received: 20 May 2021 / Received in revised form: 9 February 2022 / Accepted: 11 February 2022 / Published online: 28 February 2022

Abstract- This paper investigates the influence of grain size reduction, from 120 to 5 µm, on the electrochemical response of Fe-18.5% Cr ferritic stainless steel in 0.01 M NaOH alkaline solution. To analyze the electrochemical characteristics of the material, the potentiodynamic polarization, open circuit potential measurement, cyclic voltammetry, electrochemical impedance spectroscopy, and Mott-Schottky analysis were carried out. Open circuit potential analysis demonstrated that the passive layer developed on a coarse-grained sample is more stable than a fine-grained one. Based on electrochemical impedance spectroscopy measurements, it was concluded that grain refinement reduces the thickness of the passive protective layer and degrades the corrosion resistance of material. Polarization measurements showed that refinement of grain structure reduces the corrosion resistance of the investigated ferritic stainless steel exposed to NaOH solution. The Mott-Schottky analysis demonstrated that the protected layer formed on the surface of the fine-grained sample has donor and acceptor densities (2.43×10^{21}, and 0.4×10^{21} cm^{-3}, respectively) higher than that formed on the surface of the coarse-grained counterpart (2.29×10^{21}, and 0.36×10^{21} cm^{-3}, respectively).

Keywords- Ferritic stainless steel; Grain refinement; Electrochemical properties; EIS measurement; Mott-Schottky analysis

1. INTRODUCTION

There are different methods that can be used to improve the mechanical properties of metallic materials, including severe plastic deformation and thermomechanical processing. Numerous studies have been conducted regarding the effect of grain refinement on the mechanical properties of metals and alloys [1-4]. Grain refinement also affects the electrochemical behavior of the material. Therefore, the positive and negative influence of grain size reduction on the corrosion resistance and electrochemical response of materials have been investigated by different authors [5-8]. There are many studies regarding the effect of grain size reduction on the electrochemical behavior of austenitic stainless steel [9,10]. For example, Zheng et al. [11] elucidated that the corrosion resistance of AISI 304 austenitic stainless steel, in a 0.5 M H2SO4 solution, can be improved by grain refinement. Refai et al. [12] reported that grain refinement increases the pitting potential of Fe-20Cr stainless steel in a 1 M NaCl solution. It was also demonstrated by Scino et al. [13] that the rate of electrochemical reactions of low nickel-high nitrogen austenitic steels in 5% wt. H2SO4 solution enhances with grain size reduction. Ferritic stainless steels are a suitable and inexpensive substitute for many austenitic stainless sheets of steel due to their high strength and ductility, along with outstanding corrosion resistance in acidic and chloride solutions [14]. Ferritic stainless steels have higher chromium content than other types of stainless steel. Typically, the concentration of the chromium element in the chemical composition of the ferritic stainless steel is in the range of 12 to 27 wt. % [15]. Annealed ferritic stainless steels are very soft and ductile and possess excellent formability [16]. Ferritic stainless steels are much stronger than plain carbon steels in annealed conditions. Inspection of the available literature reveals the effect of grain refinement, by cold rolling and subsequent recrystallization annealing, on the corrosion resistance and electrochemical behavior of Fe-18.5%Cr ferritic stainless steel in NaOH solution has not been investigated. Hence, in the present investigation, the Fe-18.5% Cr ferritic stainless steel was subjected to recrystallization annealing to refine the ferrite grains in the material's microstructure. After the grain refinement process, the electrochemical behaviors of coarse and fine-grained ferritic stainless steels were evaluated and compared using the OCP analysis, potentiodynamic polarization, cyclic voltammetry, Mott-Schottky analysis, and ESI measurements.

2. EXPERIMENTAL SECTION

2.1. Materials

Table 1 shows the chemical composition of the Fe-18.5%Cr ferritic stainless steel used in the current investigation. This material was received in the form of a hot-rolled plate. The microstructure of as-received material consisted of equiaxed ferrite grains with a mean size of 120μm. To investigate the impact of grain size reduction on the corrosion behavior of the Fe-

18.5%Cr ferritic stainless steel, the microstructure was refined to an average grain size of 5μm using the proposed thermo-mechanical treatment.

Table 1. Chemical composition of the ferritic stainless steel used in the present study (Wt. %).

C	Cr	Ni	Mn	Si	N	Fe
0.04	18.5	0.06	0.13	0.8	0.05	Bal.

2.2. Thermo-mechanical processing

The high percentage of chromium in ferritic stainless steels makes the ferrite phase stable over an extensive temperature range. As a result, in this type of steel, the austenite transformation to ferrite does not occur. Therefore, the only effective way to reduce the ferrite grain size in these steels is cold working and recrystallization annealing. Figure 1 represents the schematic of the thermo-mechanical processing route executed in the present investigation to produce fine-grained ferritic stainless steel. The utilized thermo-mechanical treatment consists of three different stages. Stage 1 is the solution annealing at 1200°C for 7200s. Solution annealing produces an initial coarse-grained material with uniform chemical composition. Stage 2 was the cold rolling of the material to about 90% thickness reduction to make heavily cold worked sample. Stage 3 was the recrystallization annealing at 800°C for 180 s. The sample was quenched in water immediately after annealing to suppress grain coarsening.

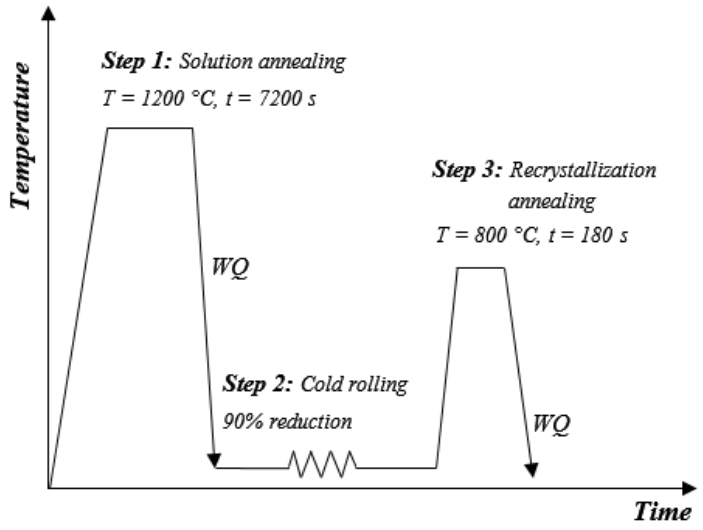

Figure 1. Schematic of the thermo-mechanical processing for the production of fine-grained sample

2.3. Electrochemical analysis

To evaluate the corrosion resistance of coarse-grained and fine-grained ferritic stainless steel, the sample's surface was finely ground using silicon carbide abrasive papers up to 3000

number. After grinding, samples were ultrasonically cleaned for 15 min in ethanol solution and then dried with air blowing. Electrochemical tests were executed in a conventional three-electrode flat cell using an Ag/AgCl electrode (in a saturated KCl solution) as a reference electrode, platinum as a counter electrode, and samples as a working electrode. The μAutolab Type III/FRA2 device equipped with Nova software was used to perform electrochemical tests. Samples were immersed in 0.01 M NaOH solution to reach steady corrosion potentials, then the potentiodynamic tests were executed in the potential range of -200 to 1200 mv vs. OCP. Electrochemical impedance spectrometer tests were carried out at a frequency range of 10 MHz to 100 kHz with a 10-mV amplitude under open circuit potential conditions. After the electrode stabilization at open circuit potential (OCP), the potential was swept in the cathodic direction from the initial potential of 0.65 V Ag/AgCl to the final potential of −0.65 V Ag/AgCl. Cyclic voltammetry (CV) tests were conducted between –0.2 V and 0.6 VAg/AgCl at a scan rate of 50 mVs^{-1}. It is worth noting that the selected scan range potential for all the CV tests lay in the anodic branch of the polarization curve of the alloy. Also, samples were immersed in 0.01 M NaOH solution before each electrochemical analysis to reach a steady-state corrosion potential.

3. RESULTS AND DISCUSSION

3.1. Microstructure of samples

Microstructures of the coarse-grained and thermo-mechanically treated fine-grained ferritic stainless steels are represented in Figure 2. As it is seen, the coarse-grained microstructure of as-received material (Figure 2 (a)) comprises equiaxed ferrite grains with an average grain size of 120 μm. Figure 2 (b) shows the optical microscope image of a fine-grained specimen prepared by cold rolling and subsequent recrystallization annealing. Cold rolling causes the ferrite grains to be elongated and aligned in a rolling direction. Cold rolling at ambient temperature increases the dislocation density inside ferrite grains which act as a driving force for static recrystallization when the material is heated after plastic deformation. Static recrystallization is thermal activated process and proceeds by nucleation of dislocation free grains inside the heavily cold worked microstructure.

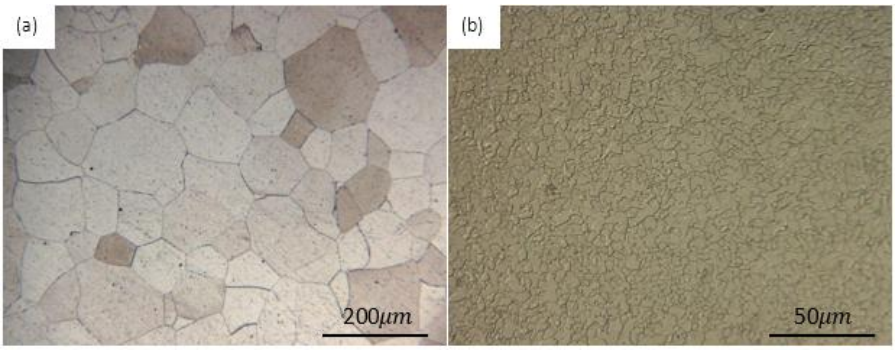

Figure 2. Microstructures of coarse-grained (a), and fine-grained (b) ferritic stainless steel

After the nucleation stage, the grains grow by moving the grain boundaries towards the cold worked microstructure, which contains a high density of dislocations. Static recrystallization is completed as the grain boundaries come together, resulting in a dislocation-free equiaxed grain structure. As can be seen in Figure 2(b), the fine-grained ferritic stainless steel resulted from the occurrence of static recrystallization with a mean grain size of about 5μm.

3.2. Open-circuit potential measurements

The OCP curves of the fine and coarse-grained steel in the NaOH solution are shown in Figure 3. As it is evident, both curves have the same behavior, which over time, the potential increases to positive values. It shows that the passive film forms on the surface of Fe-18.5% Cr steel. Also, the OCP curve of the coarse-grained sample has more positive values than the fine-grained one, which indicates that the more stable passive layer is developed on the surface of the coarse-grained specimen [17,18].

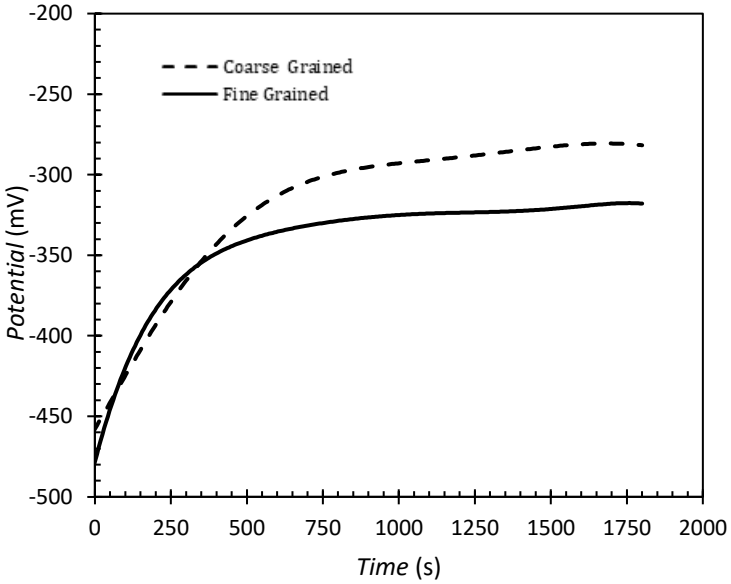

Figure 3. The OCP curves of fine and coarse grained steel in 0.1 M NaOH solution

3.3. Potentiodynamic polarization measurements

The potentiodynamic polarization curves are shown in Figure 4. As can be seen, the fine-grained and coarse-grained curves are similar, and grain refinement didn't affect pitting potential. But grain refinement has reduced the corrosion potential and increased corrosion current density. Therefore, it is concluded that the reduction of grain size has degraded the corrosion resistance in the NaOH solution. Besides, the corrosion potential is diverse from the open circuit potential, which is likely resulted from the partial evacuation of the passive layer

developed on the surface of the steel during the scanning of the potential from the negative values relative to the open circuit potential (cathodic region) [19].

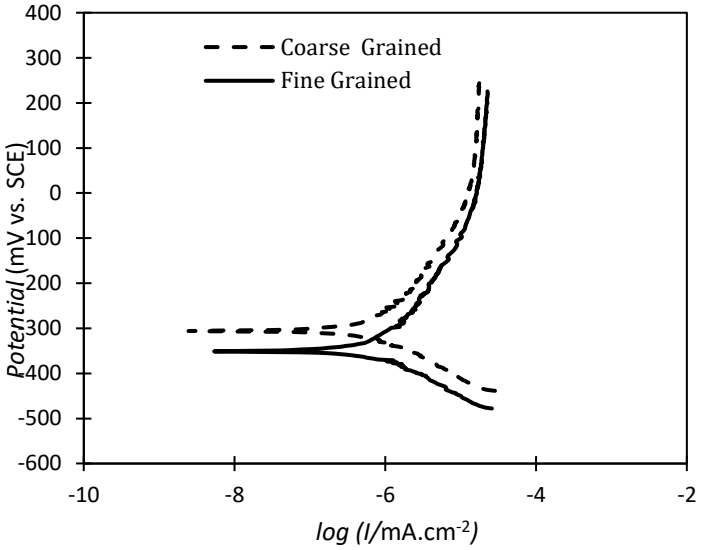

Figure 4. Potentiodynamic polarization curves of coarse-grained and fine-grained samples in 0.1 M NaOH solution

3.4. Cyclic voltammetry

The cyclic voltammetry for both samples in 0.01 M NaOH solution is represented in Fig 5. As it is evident, the loop obtained for the fine-grained sample is more extensive than for the coarse-grained one. In other words, the cathodic and anodic current density for the coarse-grained sample is lower than the fine-grained one. Therefore, the resistance of the passive film cannot be improved by grain refinement.

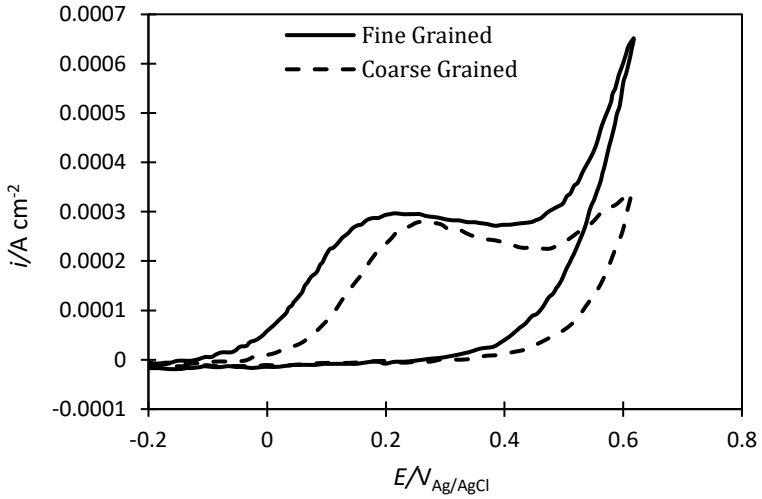

Figure 5. Cyclic Voltammograms (CV) of coarse grained and fine grained ferritic stainless steel in 0.1 M NaOH solution.

3.5. ESI measurements

The electrochemical impedance spectroscopy (EIS) analysis was conducted under the open-circuit potential conditions in the 0.01 M NaOH solution. The Nyquist, Bode, and phase curves obtained from these measurements are shown in Figure 6.

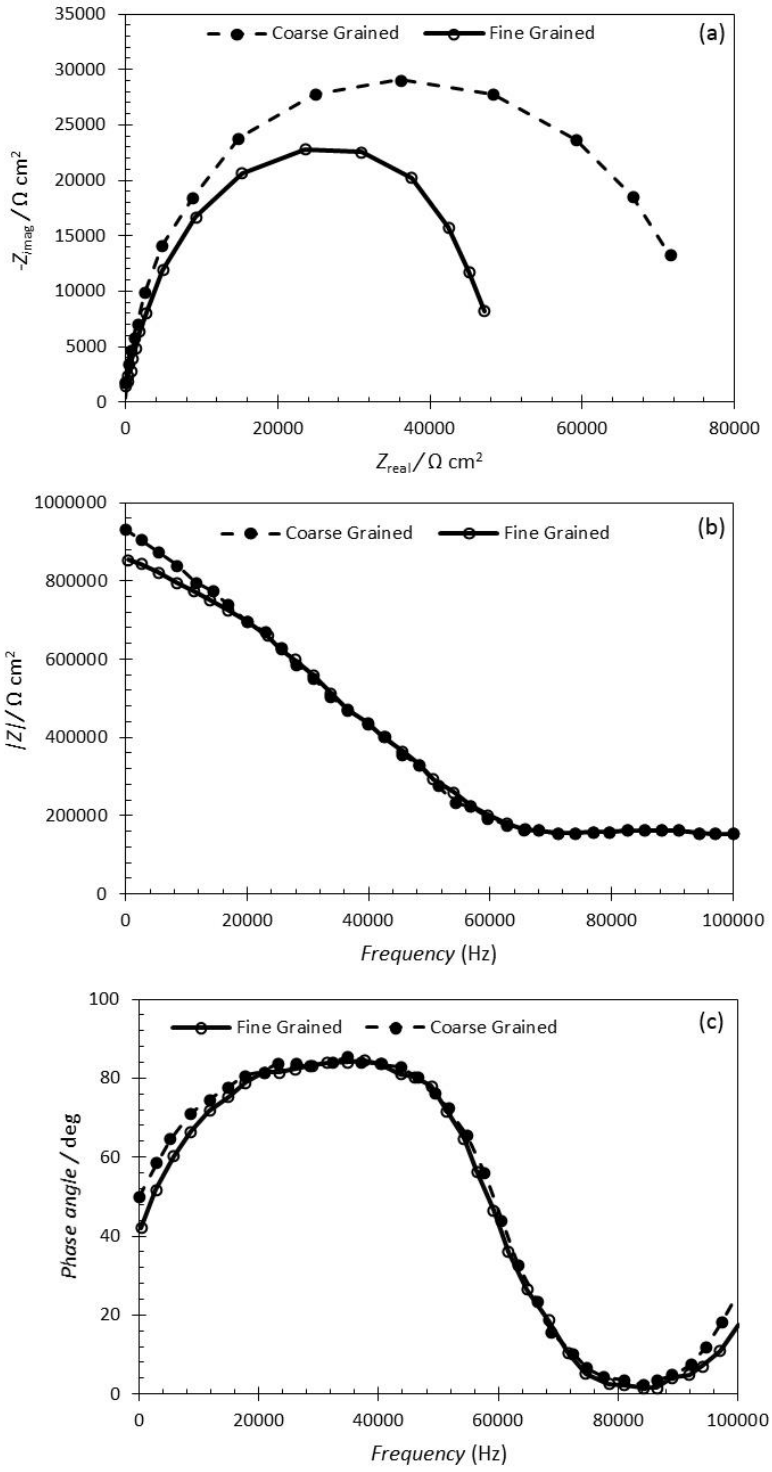

Figure 6. Nyquist (a), bode (b), and phase (c) curves of coarse-grained and fine-grained samples in 0.1M NaOH solution

To analyze the results from the impedance spectra, the electrical equivalent circuit of Figure 7 was adapted using the ZView software. In this figure, CPE is the constant phase element, R_{sol} is the solution resistance, and R_p is the polarization resistance. The Nyquist curves are shown in Figure 6(a) are both identical. It is evident that the semicircle diameter for the coarse-grained specimen is larger than the fine-grained one. This result demonstrates that the weaker passive film is developed on the surface of the fine-grained sample in comparison with the coarse-grained counterpart. The values acquired from the electrochemical impedance spectroscopy test using the proposed equivalent circuit are shown in Table 2. Hence, it is concluded that the thickness of the passive film decreases, and the corrosion resistance of material degrades by grain refinement.

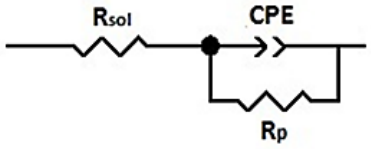

Figure 7. Equivalent circuit for fitting the electrochemical impedance spectra

Table 2. Values of the fitted impedance parameters for coarse and fine-grained samples in the 0.01M NaOH solution

Sample	R_P ($K\Omega.cm^2$)	Y_{0CPE} ($\mu F.cm^{-2}$)	R_{sol} ($\Omega.cm^2$)
Coarse- grained	31.3	33.2	4.76
Fine- grained	20.1	34.7	4.89

The following equation was utilized to calculate the thickness of the passive films developed on the surface of coarse and fine-grained samples in the 0.01 M NaOH solution [20]:

$$L_{ss} = (\varepsilon\varepsilon_0) / c \qquad (1)$$

where L_{ss} is the steady-state passive layer thickness, c is the capacitance of the passive layer, ε is the dielectric constant of the passive layer formed on iron (ε=12), and ε_0 is the vacuum permeability (8.854×10-14 F/cm). This equation reveals that the thickness of the passive layer developed on the surface of ferritic stainless steel is inversely related to the layer's capacitance. The passive layer capacitance is measured by Mott-Schottky analysis in the later section. Results of the Mott-Schottky analysis in conjunction with the above equation demonstrate that the fine-grained sample has a thinner passive layer than the coarse-grained counterpart due to the higher capacitance. Whereas, the polarization resistance of the fine-grained sample is lower than that of the coarse-grained one. So, the lower polarization resistance and the thinner passive layer in the fine-grained sample demonstrate the formation of a layer with lower resistance and

protective properties. Therefore, the main conclusion is that grain refinement does not improve the corrosion resistance and passive film properties of the Fe-18.5% Cr ferritic stainless steel in the alkaline solution.

3.6. Mott-Shottky analysis

When the stainless steel is exposed to an aqueous solution, the passive film is formed on its surface. Generally, the passive film has a crystal structure containing point defects. The presence of point defects in the passive film makes them have a semiconducting behavior [21,22]. Based on the point defect model (PDM), oxygen vacancies and metal interstitials (electron donors) act as an n-type semiconductor, and a cation vacancy (electron acceptor) acts as a p-type semiconductor in the passive film [23,24]. The Mott-Schottky analysis is a potent method to determine the semiconducting behavior of the passive layers formed on the surface of metallic materials. The equation of the Mott-Schottky analysis for n-type and p-type behavior are as follow [25]:

$$\frac{1}{C_{SC}^2} = \frac{2}{\varepsilon\varepsilon_0 e N_D}\left(E - E_{FB} - \frac{k_B T}{e}\right) \qquad (2) \qquad for\ n-type\ semiconductor$$

$$\frac{1}{C_{SC}^2} = -\frac{2}{\varepsilon\varepsilon_0 e N_A}\left(E - E_{FB} - \frac{k_B T}{e}\right) \qquad (3) \qquad for\ p-type\ semiconductor$$

where ε is the dielectric constant of the passive layer (ε=12 [26]), ε_0 is vacuum permeability (8.854×10^{-14} F/cm), k_B is the Boltzmann constant (1.38×10^{-23} J/K), T is the absolute temperature, e is the electron charge, N_D and N_A are the donor and acceptor density (cm^{-3}), E_{FB} is the flat band potential, C_{SC} is the space-charge capacitance. When the space-charge capacitance (C_{SC}) is much smaller than the Helmholtz capacitance (C_H), the interfacial capacitance (C) is equal to the space-charge (C_{SC}). The interfacial capacitance (C) is obtained using the following expression [27]:

$$C = -\frac{1}{\omega Z_{img}} \qquad (4)$$

where Z_{img} is the imaginary part of the impedance, and $\omega=2\pi f$ is the angular frequency. Figure 8 represents the Mott-Schottky curves of the fine-grained and coarse-grained Fe-18.5%Cr ferritic stainless steel in the alkaline solution. It is seen that the Mott-Schottky plots have positive slopes in the potential range of -0.7-0.3, and the negative slope in the range of 0.3-0.7. The positive and negative slopes indicate that the passive film on the Fe-18.5%Cr steel has the n-type and the p-type semiconducting behavior, respectively. The donor and acceptor densities are calculated from the negative and positive slopes of the curves shown in Fig. 8. The calculated donor and acceptor densities are shown in Table. 3. It is evident that the donor and

acceptor densities of passive films formed on the surface of the fine-grained sample are higher than the coarse-grained counterpart.

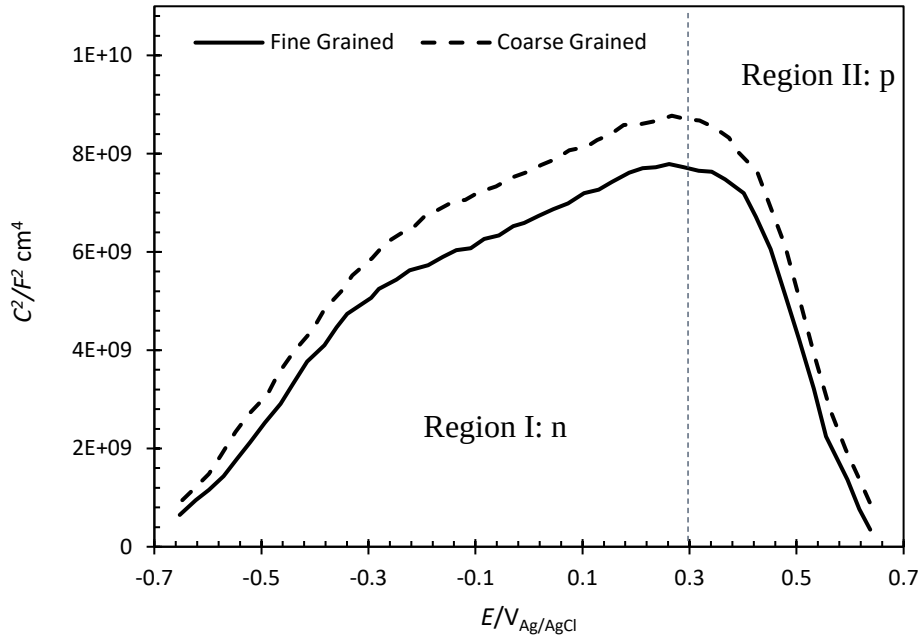

Figure 8. Mott–Schottky plots of coarse-grained and fine-grained specimens in 0.1 M NaOH

Therefore, it is seen that grain refinement lowers the density of point defects in the passive films of Fe-18.5%Cr ferritic stainless steel exposed to an alkaline solution. This behavior results in the improvement of electron transfer from the material into the electrolyte and losing the passivation resistance. It is worth noting that fine-grained stainless steels exhibit higher corrosion resistance and passivation behavior in acidic solutions [11,28]. The main cause of this phenomenon is that the surface of the fine-grained samples becomes enriched faster in chromium oxide in contact with acidic solutions. In contrast, when the material is exposed to alkaline solutions, the chromium is depleted more quickly from the sample's surface, and the weaker passive film is formed.

Table 3. Calculated donor and acceptor densities of fine-grained and coarse grained sample

Sample	Donor 1 (cm^{-3})	Donor 2 (cm^{-3})	Acceptor (cm^{-3})
Fine grained	0.89×10^{21}	2.43×10^{21}	0.4×10^{21}
Coarse grained	0.79×10^{21}	2.29×10^{21}	0.36×10^{21}

4. CONCLUSION

In the present investigation, the grain size of the Fe-18.5% Cr ferritic stainless steel was reduced from 120 to 5 μm using cold deformation and recrystallization annealing. The effect

of grain refinement on electrochemical properties was investigated by comparing the response of coarse-grained and fine-grained material to different electrochemical analyses. Following is the main results of the present study:

1-The OCP measurements showed that the curve of the coarse-grained sample has more positive values than the fine-grained one. This result demonstrates that passive film formed on the coarse-grained sample is more stable than the fine-grained one .

2- The potentiodynamic polarization measurements showed that grain refinement had reduced the corrosion resistance of Fe-18.5 Cr ferritic stainless steel in the NaOH solution .

3- The cyclic voltammetry indicated that the resistance of the passive film is not improved by grain refinement .

4- ESI measurements also proved that grain refinement reduces the thickness of the passive film and degrades the corrosion resistance.

REFERENCES

[1] S. Miran, Int. J. Mater. Sci. 4 (2014) 99.
[2] Y. Zhu, R. Z. Valiev, T. G. Langdon, N. Tsuji, and K. Lu, MRS Bulletin. 35 (2010) 977.
[3] R. Z. Valiev, Y. Estrin, Z. Horita, T. G. Langdon, M. J. Zechetbauer, and Y. T. Zhu, JOM 58 (2006) 33.
[4] F. J. Humphreys, P. B. Prangnell, and R. Priestner, Curr. Opin. Solid. State. Mater. Sci 5 (2001) 15.
[5] M. Rifai, H. Miyamoto, and H. Fujiwara, IOP Conference Series: Materials Science and Engineering, IOP Publishing 63 (2016) 120.
[6] A. Di Schino, and J. Kenny, J. Mater. Sci. Lett. 21 (2002) 1969–.
[7] A. Barbucci, M. Delucchi, M. Panizza, M. Sacco, and G. Cerisola, J. Alloys. Compd. 317-318 (2001) 607.
[8] B. Ravi Kumar, R. Singh, B. Mahato, P. K. De, N. R. Bandyopadhyay, and D. K. Bhattacharya, Mater. Charact. 54 (2005) 141.
[9] T. Balusamy, S. Kumar, and T. S. Narayanan, Corros. Sci. 52 (2010) 3826.
[10] A. Di Schino, and J. Kenny, J. Mater. Sci. lett. 21 (2002) 1631.
[11] Z. Zheng, Y. Gao, Y. Gui, and M. Zhu, Corros. Sci. 54 (2012) 60.
[12] M. Rifai, H. Miyamoto, and H. Fujiwara, IOP Conference Series: Materials Science and Engineering, IOP Publishing (2014) 120.
[13] A. Di Schino, and J. Kenny, J. Mater. Sci. Lett. 21 (2002) 1969.
[14] M. O. H. Amuda, and S. Miridha, Adv. Mat. Res. 83-86 (2009) 1165.
[15] S. V. Mehtonen, L. P. Karjalainen, and D. A. Porter, Mat. Scie. Eng. A 607 (2014) 44.
[16] M. Y. Huh, and O. Engler, Mat. Sci. Eng. A 308 (2001) 74.
[17] V. Moura, L. Lima, J. Pardal, A. Kina, R. Corte, and S. Tavares, Mater. Charact. 59 (2008) 1127.

[18] E. E. Oguzie, J. Li, Y. Liu, D. Chen, Y. Li, K. Yang, and F. Wang, Electrochim. Acta 55 (2010) 5028.
[19] D. Mareci, S. I. Strugaru, C. Munteanu, G. Bolat, and R. M. Souto, Int. J. Mater. Res. 106 (2015) 267.
[20] E. Sikora, and D. D. Macdonald, Solid. State. Ion 94 (1997) 141.
[21] R. M. Fernandez-Domene, E. Blasco-Tamarit, D. M. Garcia-Garcia, and J. Garcia-Anton, Thin. Solid. Films 558 (2014) 252.
[22] A. Fattah-alhosseini, M. Golozar, A. Saatchi, and K. Raeissi, Corros. Sci. 52 (2010) 205.
[23] S. Yang, and D. D. Macdonald, Electrochim. Acta. 52 (2007) 1871.
[24] Y. Zhang, M. Urquidi-Macdonald, G. R. Engelhardt, and D. D. Macdonald, Electrochim. Acta 69 (2012) 1.
[25] S. R. Morrison, Electrochemistry at Semiconductor and Oxidised Metal Electrodes, Plenum Press, New York (1980).
[26] R. Babic´, M. Metikoš-Hukovic´, J. Electroanal. Chem. 358 (1993) 143.
[27] E. Sikora, and D. D. Macdonald, Electrochim. Acta. 48 (2002) 69.
[28] A. Fattah-alhosseini, and S. Vafaeian, J. alloys. Compd. 639 (2015) 301.